

21GRD05 Met4H2

D1 – Report on the assessment of different methods to establish traceability for the measurement of hydrogen leak rates flowing to atmosphere in the range  $10^{-9}$  mol/s to  $10^{-6}$  mol/s

Organisation name of the lead participant for the deliverable: CNAM

Due date of the deliverable: 31 July 2025

Actual submission date of the deliverable: 5 November 2025

---

**Confidentiality Status:** PU - Public, fully open

**Deliverable Cover Sheet**

Funded by the European Union. Views and opinions expressed are however those of the author(s) only and do not necessarily reflect those of the European Union or EURAMET. Neither the European Union nor the granting authority can be held responsible for them.

The project has received funding from the European Partnership on Metrology, co-financed from the European Union's Horizon Europe Research and Innovation Programme and by the Participating States.

European Partnership  Co-funded by the European Union

**METROLOGY  
PARTNERSHIP**



Task 1.1	Activity 1.1.7	Reporting date 09.09.2025
Title Report on the assessment of different methods to establish traceability for the measurement of hydrogen leak rates flowing to atmosphere in the range $10^{-9}$ mol/s to $10^{-6}$ mol/s		
Authors Frédéric Boineau (LNE), Primož Žibret (UL), Gregor Bobovnik (UL), Jože Kutin (UL), Zaccaria Silvestri (CNAM), Jean-Pierre Wallerand (CNAM), Martin Vičar (CMI)		Corresponding author Frédéric Boineau LNE
Contributing partners CMI, CNAM, LNE, UL		
Key words Leak rate measurement, Constant-pressure flowmeter, Constant-volume flowmeter, PVTt system, Refractometry		
Notice This work was funded by the European Union. Views and opinions expressed are however those of the author(s) only and do not necessarily reflect those of the European Union or EURAMET. Neither the European Union nor the granting authority can be held responsible for them. The contents of this report have been obtained using best scientific practices and have been peer-reviewed prior to release. Nevertheless, the material is provided “as is”, without any kind of warranty regarding correctness, completeness, or fitness-for-purpose.		
Acknowledgement The project Met4H2 21GRD05 has received funding from the European Partnership on Metrology, co-financed from the European Union’s Horizon Europe Research and Innovation Programme and by the Participating States.		
DOI n/a	License CC-BY-4.0	Copyright © The authors
Feedback The consortium welcomes feedback. Please send your comments, suggestions or other feedback to the project coordinator, Dr. Adriaan van der Veen (VSL), <a href="mailto:avdveen@vsl.nl">avdveen@vsl.nl</a> .		

## Summary

The aim of this task is to provide the traceability of leak flow rates, with reference to atmospheric pressure, at typical flow rates from  $10^{-6}$  mol/s to  $10^{-9}$  mol/s. Leak detectors are typically checked by means of leak artefacts and these should be calibrated using a traceable gas flowmeter.

The gas flowmeters and techniques that will be developed in this task are complementary in their range of measurement, with an overlap in the decade of  $10^{-7}$  mol/s, and also in their measurement technique. A cross validation of the flowmeters is therefore possible and will be undertaken in this task.

## Contents

21GRD05 Met4H <sub>2</sub> .....	1
Summary .....	3
1 Introduction .....	5
2 Transfer standards .....	5
3 Participants and standards .....	5
3.1 CMI - Czech Republic .....	6
<b>3.1.1 Laminar flow element .....</b>	<b>6</b>
<b>3.1.2 Constant pressure flowmeter .....</b>	<b>6</b>
<b>3.1.3 Operation during the L1 a L2 leaks comparison .....</b>	<b>8</b>
<b>3.1.4 Mutual confirmation of both developed systems .....</b>	<b>9</b>
<b>3.1.5 Limitations of the systems .....</b>	<b>9</b>
3.2 CNAM - France .....	10
<b>3.2.1 Description of the measurement principle .....</b>	<b>10</b>
<b>3.2.2 Experimental setup .....</b>	<b>11</b>
<b>3.2.3 First results and first estimation of uncertainties .....</b>	<b>12</b>
3.3 LNE - France .....	13
<b>3.3.1 Calibration setup .....</b>	<b>14</b>
<b>3.3.2 L1 calibration with the low-range configuration .....</b>	<b>15</b>
<b>3.3.3 L2 calibration with the high-range configuration .....</b>	<b>15</b>
<b>3.3.4 Calibration uncertainty .....</b>	<b>16</b>
3.4 UL - Slovenia .....	17
4 Characterisation of the transfer standards .....	19
4.1 Sensitivity to the upstream pressure .....	19
4.2 Sensitivity to the downstream pressure .....	20
4.3 Sensitivity to the temperature .....	20
4.4 Stability over time .....	21
4.5 Internal volume .....	22
5 Schedule of the comparison .....	23
6 Calibration procedure for the comparison .....	24
6.1 Quantity to be determined .....	24
6.2 General procedure .....	24
<b>6.2.1 Temperature .....</b>	<b>24</b>
<b>6.2.2 Downstream pressure .....</b>	<b>24</b>
<b>6.2.3 Upstream pressure .....</b>	<b>24</b>
<b>6.2.4 Number of measurements .....</b>	<b>24</b>
<b>6.2.5 Summarised operating mode .....</b>	<b>24</b>
7 Comparison results .....	25
7.1 Set of measurements .....	25
7.2 Reducing the results .....	25
7.3 Results for L1 .....	26
7.4 Results for L2 .....	27
8 Conclusion .....	28
Annex: Reported data of the participating laboratories and intermediate calculations .....	30

## 1 Introduction

National metrology institutes belonging to the working groups Fluid flow, Pressure and vacuum and Length of the BIPM (Bureau international des poids et mesures) have developed primary standards to measure hydrogen leak rates flowing at atmospheric pressure. To assess these standards, a comparison was organised using two transfer standards allowing leak rates of hydrogen over the range  $3 \times 10^{-9}$  mol·s<sup>-1</sup> to  $1 \times 10^{-6}$  mol·s<sup>-1</sup> (about 0.004 sccm to 1.3 sccm). The measuring standards including their uncertainty budget are described in section 3. Metrological characteristics of the transfer standards such as internal volumes, temperature coefficient and stability over the course of the comparison are presented in section 4. Finally, measurements results are presented together with the characteristics of the transfer standards such as internal volumes, temperature coefficient and stability over the course of the comparison.

## 2 Transfer standards

Two leak artefacts were necessary for the comparison. They are identified L1 and L2 and were provided by the French Manufacturer ASC Instruments. The characteristics of the transfer standards are summarized in Table 1. The nominal downstream pressure was fixed to 100 kPa,

**Table 1: Transfer standards details.**

Leak artefact Identification	Technology	Serial number	Applied upstream pressure in kPa	Nominal flow rate in mol·s <sup>-1</sup>
L1	Metal capillary	FE210514	700	$2 \times 10^{-8}$
			300	$3 \times 10^{-9}$
L2	Sintered metal	FE210515	500	$1 \times 10^{-6}$
			250	$2 \times 10^{-7}$

The transfer leak artefacts are mechanically identical (see Figure 1). The arrow etched on the metal body of the artefact indicates the flow direction. Two fittings were connected on both ends: a gender changer Swagelok 6 mm on the input and an adapter Swagelok 6 mm towards VCR®1/4 male on the output.

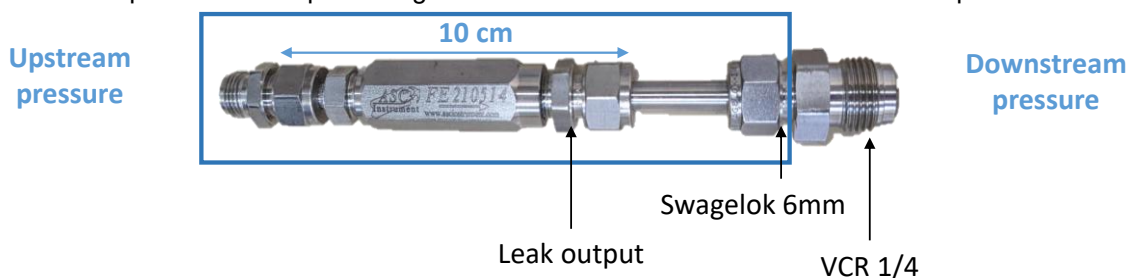


**Figure 1: Picture of the leak artefact L1 and details of the fittings.**

## 3 Participants and standards

Table 2 summarizes the standards used by the participants and indicates whether the standards are independent or not.

**Table 2: Participants standards.**

Laboratory	Standard	Traceability
CMI Czech Republic	Constant pressure flowmeter	Independent

CNAM France	Constant volume flowmeter using a Fabry-Pérot cavity for pressure measurement variation	LNE, France (internal volume calibration)
LNE (Pilot) France	Constant volume flowmeter using a conventional pressure gauge for pressure measurement variation	Independent
UL Slovenia	pVTt flowmeter	Independent

Details of the flow standards are given in the following paragraphs for each participant.

### 3.1 CMI - Czech Republic

CMI has developed a constant pressure flowmeter for the leak rates referred to atmosphere in the range ( $10^{-9}$  to  $10^{-6}$  mol/s). The existing laminar flow element Molbloc 10 sccm s/n 2986 was characterised for hydrogen in the range  $10^{-6}$  mol/s to  $10^{-5}$  mol/s using the primary gravimetric flow standard. Both flowmeters have been compared in the overlapping range.

#### 3.1.1 Laminar flow element

The 10 sccm nominal range laminar flow element Molbloc s/n 7488 has been characterised using the primary gravimetry flow system GFS.



**Figure 2. Laminar flow element Molbloc s/n 7488.**

The previously defined hydrogen gas “H<sub>2</sub>” range “HIP” with internal constants  $\{C_G = 3.042576 \cdot 10^{-17}; \beta = 2.082966 \cdot 10^{-5}; \varepsilon = 0\}$  has been used for the traceability measurements with GFS.

Average $q_{GFS}$ mol/s	Average $q_{GFS}$ cm <sup>3</sup> /min	Average $q_{MOLBLOC}$ mol/s	Average $q_{MOLBLOC}$ cm <sup>3</sup> /min	Molbloc average deviation % Reading	Expanded uncertainty % Reading	Molbloc correction [1]
$9.2612 \times 10^{-7}$	1.3683	$9.2442 \times 10^{-7}$	1.3657	-0.18%	0.38%	1.0018
$2.0883 \times 10^{-6}$	3.0852	$2.0873 \times 10^{-6}$	3.0838	-0.05%	0.29%	1.0005
$4.5432 \times 10^{-6}$	6.7121	$4.5439 \times 10^{-6}$	6.7132	0.02%	0.17%	0.9998
$1.0450 \times 10^{-5}$	15.4389	$1.0456 \times 10^{-5}$	15.4472	0.05%	0.16%	0.9995

The flowrates in table expressed in ml/min are calculated for nominal temperature 23 °C and pressure 100 kPa. The evaluated Molbloc corrections together with unchanged set of internal constants  $\{C_G; \beta; \varepsilon\}$  has been used for the following measurements.

#### 3.1.2 Constant pressure flowmeter

Constant-pressure flowmeter OMZ is consists of two pistons with nominal diameters 6 mm and 23 mm.

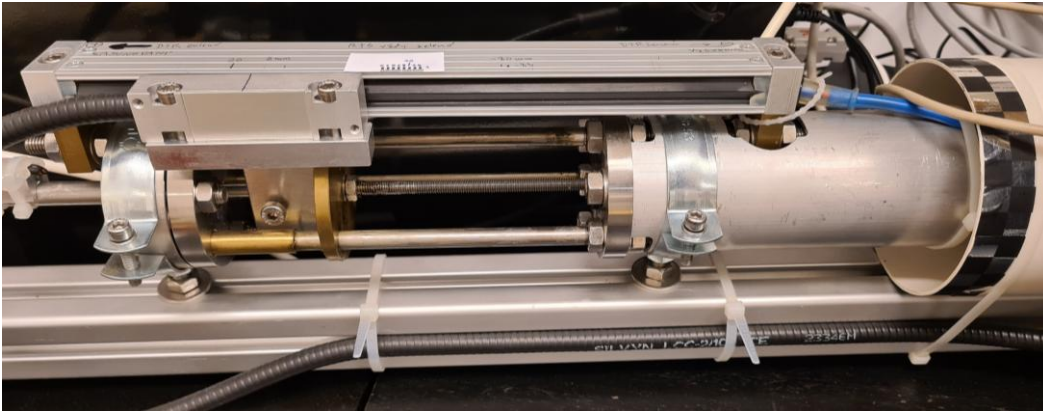


Figure 3. OMZ A: nominal diameter  $d = 23$  mm, total stroke length  $L = 250$  mm, total  $V = 100$  cm<sup>3</sup>.

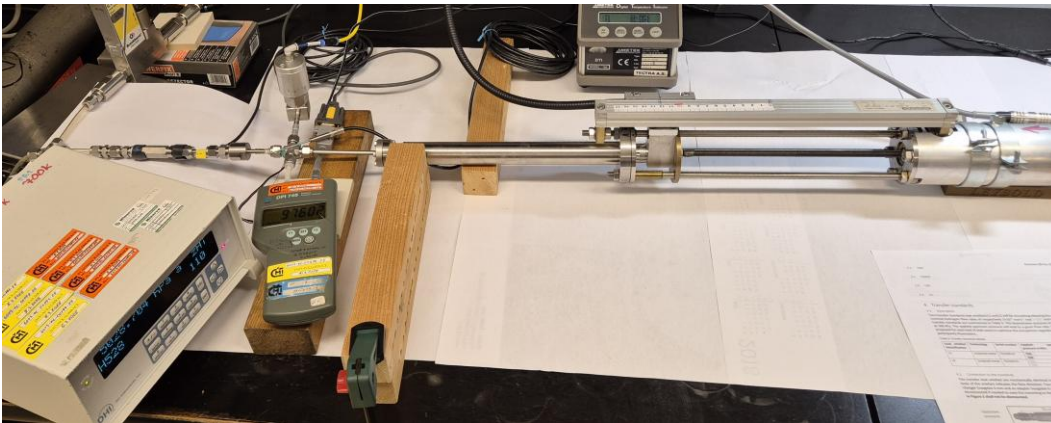


Figure 4. OMZ B: nominal diameter  $d = 6$  mm, total stroke length  $L = 100$  mm, total  $V = 2.5$  cm<sup>3</sup>.

Each piston is equipped with opto-electronic position sensing and a stepper motor ensuring the movement of the piston relative to the housing. The pistons are sealed against the housing with a Teflon seal with a rubber insert.

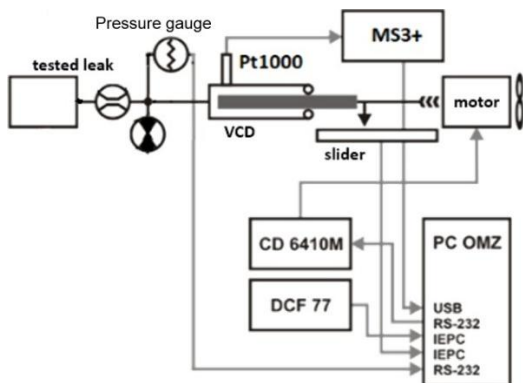


Figure 5. System schematic of the constant pressure flowmeter.

To overcome the irregularities and non-linearities of the piston position calculated directly from the stepper motor rotations, the optical ruler is used to precisely determine the piston position.

OMZ B: Range ( $2 \cdot 10^{-5}$  to  $2 \cdot 10^{-2}$ ) mbar·dm<sup>3</sup>/s is given by a time needed for one piston run over its entire stroke from 1 d 15 h to 2 min.

OMZ A: Similarly, range ( $1 \cdot 10^{-3}$  to  $5 \cdot 10^{-1}$ ) mbar·dm<sup>3</sup>/s is given by a time needed for one piston run (or at least 1/3 of full stroke) over its entire stroke and the maximum piston speed.

### 3.1.3 Operation during the L1 a L2 leaks comparison

The volume of hydrogen flowing from the measured leak into the flowmeter is compensated by continuously extending the piston from the housing.

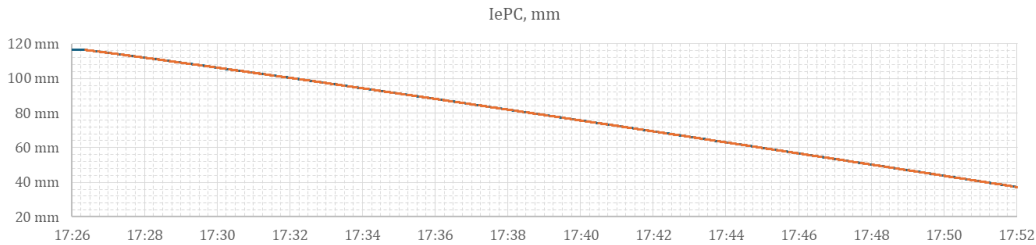


**Figure 6. The piston position over time.**

The piston position over time, the system pressure, and the temperatures of key system components are recorded.

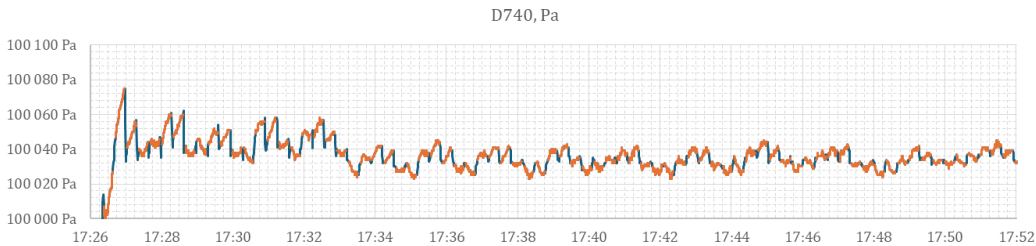


**Figure 7. The pressure gauge indication over time.**

Based on changes in pressure in the flow meter, the piston extension speed is adjusted to keep the pressure constant.

Determination of the dead volume is done at the beginning of the measurement (or separately) using several step changes in the piston position; first, a slightly higher gauge pressure in the system is intentionally set (100 Pa), the piston displacement is started so that the pressure is kept constant, and a step change in volume is performed five times. From the system reaction, it is possible to estimate the current dead volume.

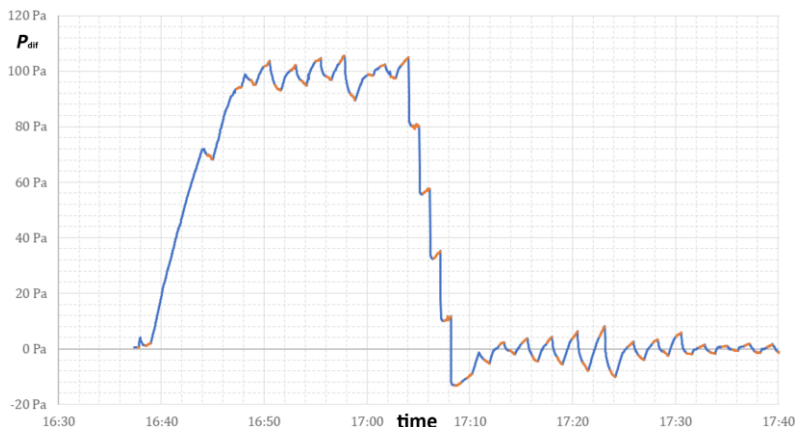


**Figure 8. Differential pressure gauge indication during the dead volume measurement.**

The volume of gas inside a closed volume converted to standard conditions is calculated as:

$$V_{STD} = [V_D + Sx_i + S(x - x_i)] \cdot \frac{p}{T} \cdot \frac{T_{STD}}{p_{STD}} \tag{1}$$

We neglect changes in compressibility. The gas flow rate converted to standard conditions (usually in the field of leaks 1 atm. or 1 bar abs. and 23 °C) is determined for measurement in the time interval  $\Delta t$  as:

$$q_{STD} = \frac{1}{\Delta t} \cdot \frac{T_{STD}}{p_{STD}} \cdot \left( [V_D + Sx_i + S(x_e - x_i)] \cdot \frac{p_e}{T_e} - [V_D + Sx_i] \cdot \frac{p_i}{T_i} \right) \quad (2)$$

Relative type-B uncertainty is given as:

$$u_{Br}(q_{STD}) = \sqrt{u_r^2(S) + u_r^2(x_e) + u_r^2(\Delta t) + u_r^2(p_e) + u_r^2(T_e) + u_r^2(C)} \quad (3)$$

Typical input values are:

$$u_r(C) = 1.6 \cdot 10^{-3}, \text{ dominated by } u_r(V_D) = 0.1$$

$$u_r(S) = 8 \cdot 10^{-4}$$

$$u_r(p_e) \leq 1 \cdot 10^{-4}, \text{ but adding compressibility changes } u_r(p_e) \leq 3.2 \cdot 10^{-4}$$

$$u_r(T_e) \leq 1.5 \cdot 10^{-4}$$

$$u_r(\Delta t) = 5 \cdot 10^{-5}$$

$$u_r(x_e) = 2.5 \cdot 10^{-5}$$

To the result  $u_{Br}(q_{STD}) = 0.18\%$  adding the uncertainty of the variance of one measurement (piston stroke) and repeatability (multiple strokes), we typically obtain for ( $k = 2$ )  $u_C(q_{STD}) = (1.4 \text{ to } 3.5)\%$  for OMZ B and  $u_C(q_{STD}) = (0.23 \text{ to } 0.9)\%$  for OMZ A.

### 3.1.4 Mutual confirmation of both developed systems

Both systems enable direct comparison of the flowrates. The hydrogen flow from the Molbloc has been set using the manual valve to overcome potential gas temperature changes arising from MFC valve. The OMZ was operated in standard way, i.e. retracting the piston to keep the pressure inside the flowmeter constant (barometric pressure).

Flowrate Setpoint cm <sup>3</sup> /min	Average $q_{MOLBLOC}$ mol/s	Average $q_{MOLBLOC}$ cm <sup>3</sup> /min	OMZ system used	Average $q_{OMZ}$ cm <sup>3</sup> /min	OMZ average deviation relative to Molbloc % Reading
1.3	$8.8372 \times 10^{-7}$	1.3056	OMZ B	1.3065	0.07%
3.0	$2.0883 \times 10^{-6}$	3.0852	OMZ A	3.0877	0.08%
5.0	$3.3988 \times 10^{-6}$	5.0214	OMZ A	5.0230	0.03%
10.0	$6.7562 \times 10^{-6}$	9.9816	OMZ A	9.9881	0.06%
15.0	$1.0203 \times 10^{-5}$	15.0744	OMZ A	15.0804	0.04%

The results (cm<sup>3</sup>/min are expressed for 100 kPa and 23 °C standard conditions) are within the expected uncertainties of both systems confirmed and doesn't differ from the results acquired during similar comparison with nitrogen and dry air.

### 3.1.5 Limitations of the systems

The measurements and comparisons performed revealed the following sources of uncertainty, which can be further improved to reduce the overall uncertainty of the determined gas flow:

#### Temperature stabilization

The effect of temperature is compensated by continuous measurement of the temperature of parts of the system. Temperature stability given by the stability of the laboratory environment is acceptable during the day and very good during overnight measurements. Active or passive stabilization of the flow meter would reduce temperature fluctuations regardless of the time of day.

#### Piston temperature

After inserting the piston, it is necessary to wait about 20 minutes before starting the next measurement for the piston temperature to stabilize, which is slightly increased by friction (up to 0.1 °C on the outer parts, probably slightly more inside the piston).

#### Other temperature sources

The electronics of the optical ruler slider also proved to be a source of heat when imaging with a thermal camera; the heat released here could also be dissipated in a similar way to the heat from the stepper motor, for example, by means of directed ventilation.

### Gas inlet pressure preparation system

Furthermore, during the experimental work, it was found that when using some industrially manufactured pressure regulators (calibrators), the gas with regulated pressure at the regulator outlet is a mixture of gas from the pressure cylinder (in this case hydrogen) and atmospheric gases, probably due to the internal arrangement of the gradual pre-regulation and regulation of the outlet pressure. It is necessary to use systems and assemblies where the possibility of atmospheric gas penetration is eliminated.

### Permeation of H<sub>2</sub>

For the lowest hydrogen flow rates, hydrogen permeation through the plastic parts (tubes) of the system is a significant additional source of uncertainty. Permeation can be measured and then systematically compensated for, while its effect can be reduced by decreasing the surface area of the plastic parts, ideally by eliminating them completely, if the design of the connected leak allows it.

## 3.2 CNAM - France

In the scope of the project Met4H<sub>2</sub>, CNAM has developed a constant volume flowmeter based on based on a Fabry-Pérot refractometer (FPR). The main objective was to demonstrate the feasibility of the measurement.

### 3.2.1 Description of the measurement principle

It consists of two parallel mirrors separated by a spacer of fixed length (Figure 9). This arrangement allows a laser beam to transmit through one mirror and undergo multiple reflections between the mirror surfaces. Constructive interference arises when the spacer length,  $L$ , equals an integer,  $q$ , times half the laser wavelength,  $\lambda/2$ . The resulting transmitted light signal is modeled by an Airy function, which represents the resonance behavior of the FP cavity's fundamental transverse electromagnetic mode (TEM<sub>00</sub>). In practice, the frequency of the laser  $\nu_l$  is adjusted to be locked on the  $k^{\text{th}}$  resonant mode of the cavity, and its expression is then written as:

$$\nu_l \approx \frac{kc}{2nL}, \quad (4)$$

where  $c$  is the speed of light in vacuum and  $n$  is the refractive index of the gas filling the cavity.

The molar density  $\rho$  can be calculated using the Lorentz-Lorenz equation (4):

$$\frac{n^2-1}{n^2+2} = \rho(A_R + B_R\rho + \dots), \quad (5)$$

with  $A_R$  the molar polarizability and the  $B_R$  the second virial coefficient of the considered gas.

If the pressure variation is weak, the molar density variation can be written:

$$\rho = \frac{2}{3A_R} \left( \frac{\Delta f}{\nu_{gas}} \right) - \frac{1}{9A_R} \left( 1 + 4 \frac{B_R}{A_R^2} \right) \left( \frac{\Delta f}{\nu_{gas}} \right)^2. \quad (6)$$

Finally, the molar flow rate  $q$  is expressed in mol.s<sup>-1</sup> as:

$$\Delta q = \frac{\Delta \rho V}{\Delta t}, \quad (7)$$

with  $t$  the time in second and  $V$  the volume of the gas in m<sup>3</sup>.

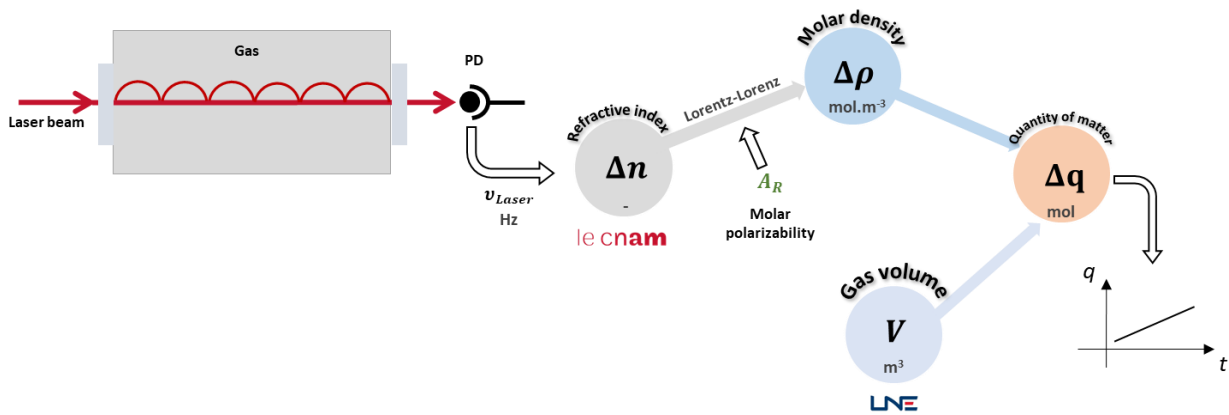


**Figure 9. Principle of the measurement using a Fabry-Perot resonator.**

The traceability of the measurement is guaranteed by unit of meter for the determination of the molar density and by LNE (France) for the internal volume calibration.

### 3.2.2 Experimental setup

The FPR can be set up as dual-FP-cavity systems (see Figure 10, Figure 11 and Figure 12). This means that the change in refractivity is practically assessed as a shift in the beat frequency between the frequencies of two lasers: one addressing the measurement cavity and the other probing the reference cavity when gas is introduced into (or evacuated from) the measurement cavity. In this case, each laser is locked to its own cavity.

The dual FP cavity, 120 mm long and 90 mm large, is made in Invar for the spacer and fused silica for the two mirrors. Each cavity consists of two 22 mm highly reflective plano-concave mirrors (99.997%) and a spacer with a 4 mm diameter hole for laser purposes. A second 17.2 mm diameter hole is present at the top of the space for gas injection. Mirrors mounting are not based on optical bonding but pressed are pressed onto the Invar spacer using O-rings and a clamping bracket. Finally, there are several holes for temperature probes.

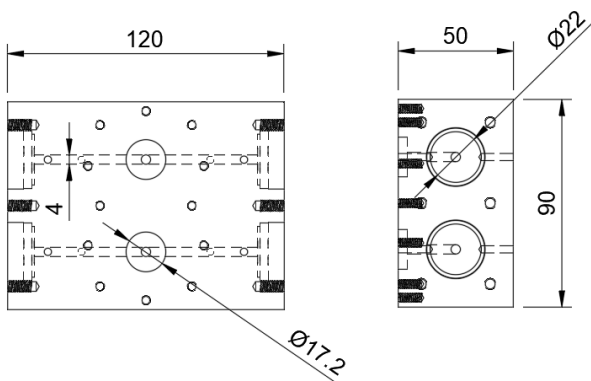


**Figure 10. Drawings of the dual FP cavity in Invar.**

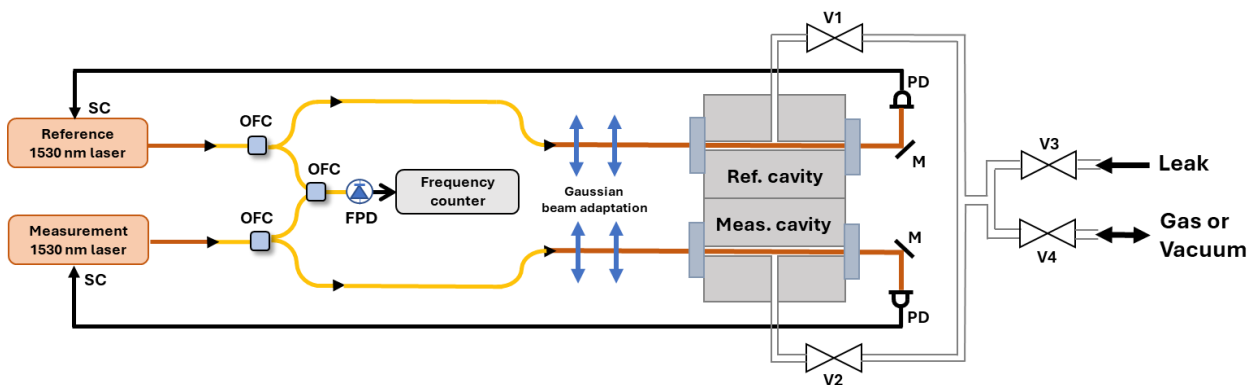


Figure 11. Experimental setup carried out at CNAM for hydrogen leak measurements composed of three main blocks: Leak artefact including Pt100 temperature sensor, dual FP cavity and Frequency. Components include optical fiber couplers (OFC), Servo-Control electronics (SC), a fast photodetector (FPD), photodiodes (PD) and pneumatic valves (VX).

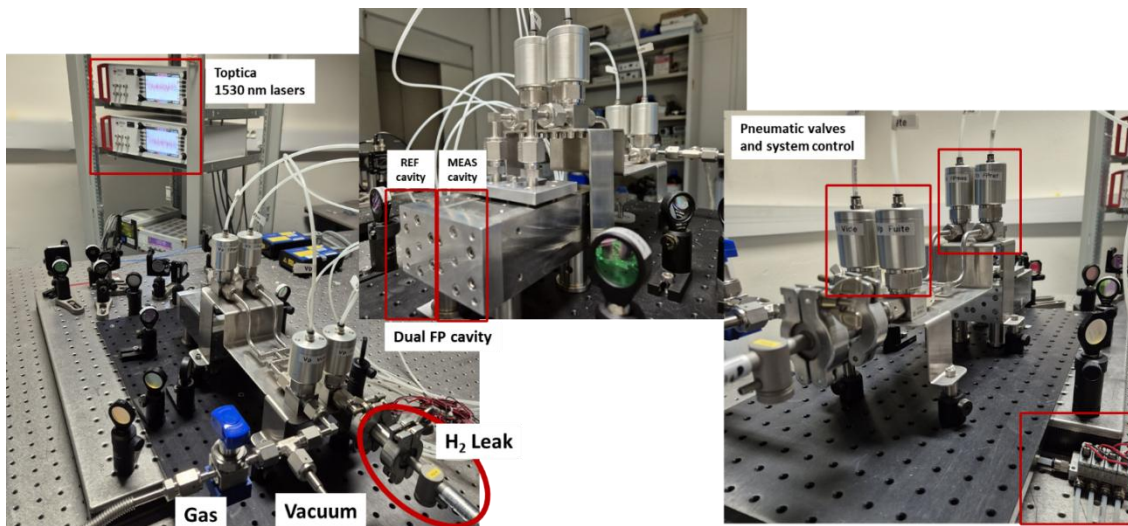


Figure 12. Pictures of the setup used at CNAM for performing hydrogen leak measurements.

The volume of the setup had been determined by LNE in the scope of the comparison including the leak artifact:  $V_{\text{FPR}+\text{Leak}} = 21.273(50) \text{ cm}^3$  at 20 °C.

Considering only the volume of the FPR:  $V_{\text{FPR}} = 19.548 \text{ cm}^3$  at 20 °C.

### 3.2.3 First results and first estimation of uncertainties

The feasibility of measuring hydrogen leak with this system has been demonstrated. Figure 13 presents an example of the variation of the molar density inside the measurement Fabry-Perot cavity when the hydrogen leak is connected to the system (the reference cavity is isolated from leak). From this plot, the estimated flow rate is about  $3.5 \times 10^{-9} \text{ mol} \cdot \text{s}^{-1}$ .

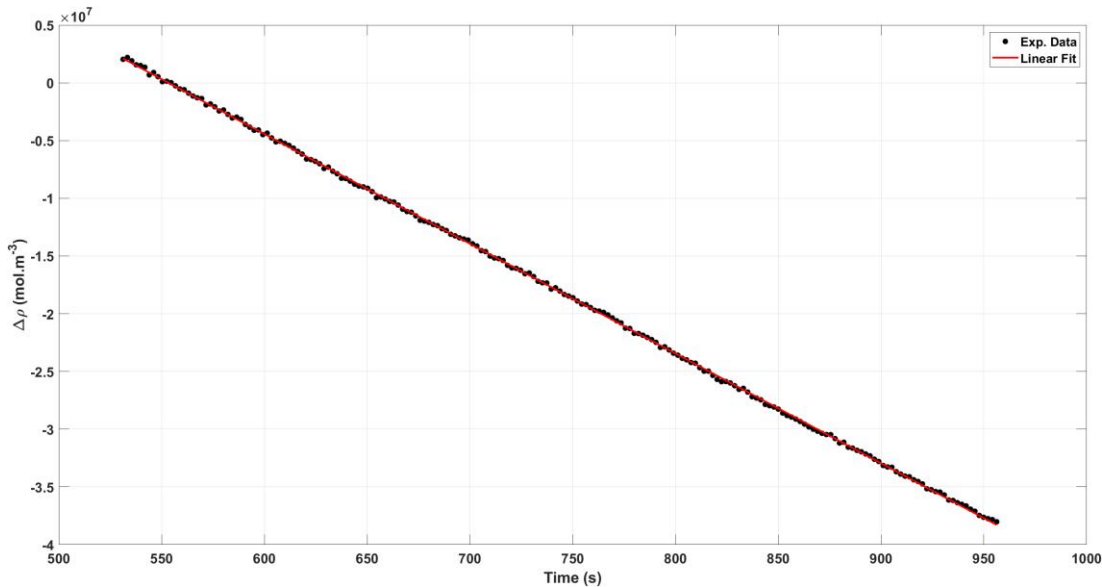


**Figure 13. Plot of the variation of the molar density when the hydrogen leak artefact is connected to the FPR systems.**

The first uncertainty budget has been established with a standard deviation of about 1%. This includes mainly the contribution of volume determination, the molar density changes over time (uncertainty fitting) and the uncertainties of both coefficients  $A_R$  and  $B_R$ .

Potential deviations from the reference value can be attributed to a potential leak in the system, or/and to poor knowledge of the coefficients  $A_R$  and  $B_R$  of hydrogen.

### 3.3 LNE - France

The flow standard of LNE, CVFM2, is in the field of vacuum metrology a so-called constant-volume and variable pressure flowmeter. It was developed in the frame of the JRP 21GRD05 to measure flow rates any type of gas at a given line pressure ranging from 20 Pa to 200 kPa. Measurements performed for the JRP are limited to hydrogen flow rates at atmospheric pressure. The measurand  $q_{pV}$  is the flow rate in pressure-volume unit and is the variation rate of the volume and the gas pressure at a constant temperature  $T$ . It is given by the definition:

$$q_{pV} = \frac{d(pV)}{dt} . \quad (8)$$

In a constant-volume flowmeter, this flow rate is thus:

$$q_{pV} = V_m \frac{dp}{dt} , \quad (9)$$

where  $V_m$  is the measurement volume. In CVFM2,  $V_m$  is composed of a standard volume  $V_{st}$  in series with a so-called dead volume  $V_d$  corresponding to the internal volumes of plumbery, valves, pressure gauges (Figure 14).

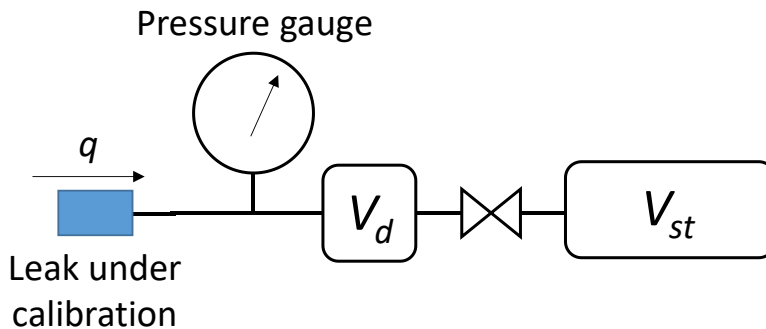


**Figure 14. General scheme of a constant-volume flowmeter**

The volume  $V_{st}$  value is obtained by a gravimetric calibration: the volume is weighed successively empty and filled with water. Knowing precisely the density of water, the value of  $V_{st}$  can be deduced with an uncertainty  $u(V_{st}) = 1 \times 10^{-4} \times V_{st}$ . The dead volume  $V_d$  is changing upon the internal volume of the leak device connected to the flowmeter and the necessary plumbrery adaptation depending on the flow range (i.e. the pressure gauges which are used).

$V_d$  is determined thanks to the flow rate of the leak under calibration in two steps:

- 1- Measurement of the pressure variation rate in  $V_d$
- 2- Measurement of the pressure variation rate in  $V_d + V_{st}$

Details of  $V_d$  calibration can be seen in [2]. There is an optimal range of the flow rate to minimise both the uncertainty of  $V_d$  and the duration of its calibration. In particular, if the flow rate to be measured is low, the time required to get a sufficient pressure variation with respect to the resolution of the pressure gauge can be long. The other issue is the pressure variation rate due to the temperature variation which leads to a residual flow rate that can be significant against the leak flow rate to be measured [3]. To overcome these problems, an auxiliary leak artefact with an optimal flow rate, connected in parallel with the leak under calibration is used; the technique is described in [3]. Once  $V_d$  is calibrated, the auxiliary leak is replaced by a blank flange. This technique relies on the precise knowledge of the physical volume occupied in  $V_m$  respectively by the auxiliary leak artefact and the blank flange.

### 3.3.1 Calibration setup

The flowmeter CVFM2 design benefits from the above-mentioned technique. Moreover, the thermal inertia and the thermal isolation of the instrument have been considered to make the residual flow rate both low and constant during several hours. The schematic of the setup in the configuration of low leak rate measurement is shown Figure 15.

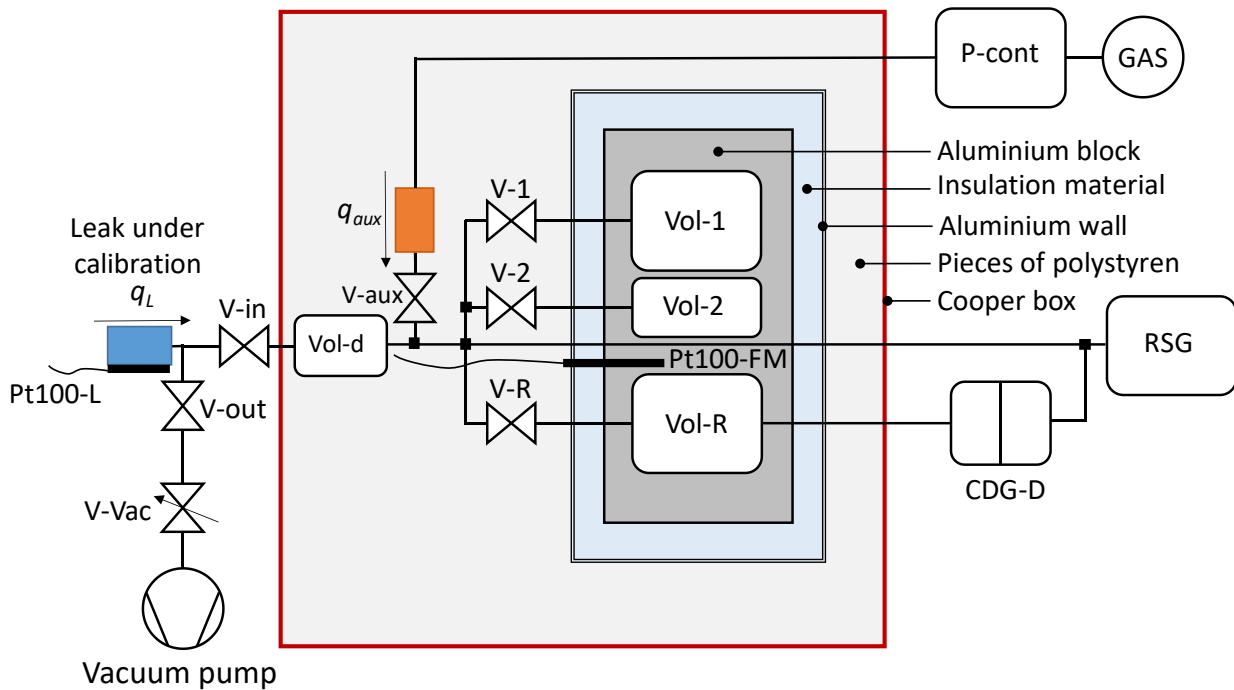


**Figure 15. Principle of the constant-volume flowmeter CVFM2 (low-range configuration).**

$q_L$ : Flow rate of the leak under calibration,  $q_{aux}$ : flow rate of the auxiliary leak artefact (capillary); **RSG**: Digital barometer; **CDG-D**: Differential capacitance diaphragm gauge of 1 kPa full scale; **P-cont**: Absolute pressure controller, 1000 kPa full scale; **Vol-1**: Standard volume of 1000 cm<sup>3</sup>; **Vol-2**: Standard volume of 200 cm<sup>3</sup> or 30 cm<sup>3</sup>; **Vol-R**: volume of 150 cm<sup>3</sup> connected to the reference port of the differential pressure gauge; **Vol-d**: Dead volume of tubing, gauges, valves, etc.; **V-1**, **V-2**, **V-R**, **V-aux**: Pneumatic bellows valves; **V-in**, **V-out**: Manual bellows valves; **V-Vac**: Adjustable micro-leak valve; **Pt100-L**: Pt100 sensor to measure the temperature  $T_L$  of the leak under calibration; **Pt100-FM**: Pt100 sensor to measure the temperature  $T_{FM}$  of the flowmeter.

The flowmeter CVFM2 was designed for flow rate measurements between  $1 \times 10^{-6}$  and  $1 \times 10^{-1}$  Pa·m<sup>3</sup>·s<sup>-1</sup> ( $4 \times 10^{-10}$  and  $4 \times 10^{-5}$  mol·s<sup>-1</sup>). The standard volumes which can be applied are Vol-1 with a value  $V_1 = 1000$  cm<sup>3</sup> and Vol-2 with values  $V_{2a} = 200$  cm<sup>3</sup> and  $V_{2b} = 30$  cm<sup>3</sup>. The latter is used to measure the lowest flow rates. The pressure variation can be measured by either the digital barometer RSG or the differential capacitance diaphragm gauge CDG-D of 1 kPa full scale. The shutting of the valve V-in allows one to measure the residual pressure variation rate. When V-in and V-out are opened, the operation of the micro-leak valve V-Vac connected to a vacuum pump allows a precise setting of the downstream pressure of the leak artefact. Two configurations of CVFM2 may be applied denoted “low-range” and “high-range”. Calibrations of the leak L1 was performed the first one and calibration of L2 with the second.

### 3.3.2 L1 calibration with the low-range configuration

The set-up is that of Fig 2. The dead volume  $V_d$  of Vol-d is first determined using an auxiliary leak with a nominal rate of  $1.5 \times 10^{-3}$  with the volume Vol-2a of 200 cm<sup>3</sup> (V-1 is closed). The pressure variation rate is measured with the RSG. Then the volume Vol-2b of 30 cm<sup>3</sup> is implemented instead of Vol-2b and a blank flange replaces the auxiliary leak (V-aux is let in open position).  $V_d$  is corrected by the difference of the volume occupied in the flowmeter by respectively the auxiliary leak artefact and the blank flange. Then, the pressure variation rate is measured alternately with V-in open and closed (residual pressure rate) by means of CDG-D. The downstream pressure is measured with the RSG gauge. Temperatures  $T_L$  (leak artefact) and  $T_{FM}$  (assumed to be the flowmeter temperature) are recorded with Pt100-L and Pt100-FM respectively.

### 3.3.3 L2 calibration with the high-range configuration

The differential pressure gauge CDG-D is removed from the flowmeter and the valve V-aux is closed. Only the volume Vol-2a of 200 cm<sup>3</sup> is used. The upstream pressure of L2 is set to 390 kPa to get a pressure rate of

about 6.5 Pa/s in the  $V_d$  determination step. Then the pressure variation rate is measured alternately with V-in open and closed (residual pressure rate) by means of the RSG gauge.

### 3.3.4 Calibration uncertainty

With the constant volume flowmeter, we measure the gas flow rate in pressure-volume unit at the gas temperature estimated by the temperature  $T_{FM}$ . The real gas law is used to get the molar flow rate  $q$ :

$$q = Z_{H_2} \frac{q_{pV}}{R \cdot T_{FM}}, \quad (10)$$

where  $R$  is the molar gas constant and  $Z_{H_2}$  is the compressibility factor of hydrogen at a pressure of 100 kPa and a temperature of 20 °C which respective values are [4][5]:

$$R = 8.31446 \text{ J} \cdot \text{mol}^{-1} \cdot \text{K}^{-1}, \quad (11)$$

$$Z_{H_2} = 1.00007. \quad (12)$$

The uncertainty of  $R$  is null and that of  $Z_{H_2}$  is considered negligible with respect to other uncertainty components.

If we denote  $\dot{p}_L$  the pressure variation rate with the leak connected to the flowmeter and  $\dot{p}_0$  the residual pressure variation rate when the leak is isolate from it, the gas flow rate  $q_{pV}$  is given from equation (9) by:

$$q_{pV} = (\dot{p}_L - \dot{p}_0) \cdot V_m. \quad (13)$$

$\dot{p}_L$  and  $\dot{p}_0$  are determined by means of the linear regression of the pressure recording with time. A single measurement, denoted  $\dot{p}_{L(i)}$  is surrounded by two residual rate measurements  $\dot{p}_{0(i-1)}$  and  $\dot{p}_{0(i+1)}$  respectively (Figure 16). The residual pressure variation rate associated to  $\dot{p}_{0(i)}$  is:

$$\dot{p}_{0(i)} = \frac{\dot{p}_{0(i+1)} + \dot{p}_{0(i-1)}}{2}. \quad (14)$$

the uncertainty of the residual rate  $\dot{p}_{0(i)}$  is (rectangular distribution):

$$u(\dot{p}_{0(i)}) = \frac{1}{\sqrt{3}} \frac{\dot{p}_{0(i+1)} - \dot{p}_{0(i-1)}}{2}, \quad (15)$$

which will be convenient to express as a ratio of  $\dot{p}_{L(i)}$ .

Three successive determinations of the leak flow rate are repeated. For each measurement, initial parameters are set to get a mean downstream pressure  $p_{down}$  as close as possible as 100 kPa.

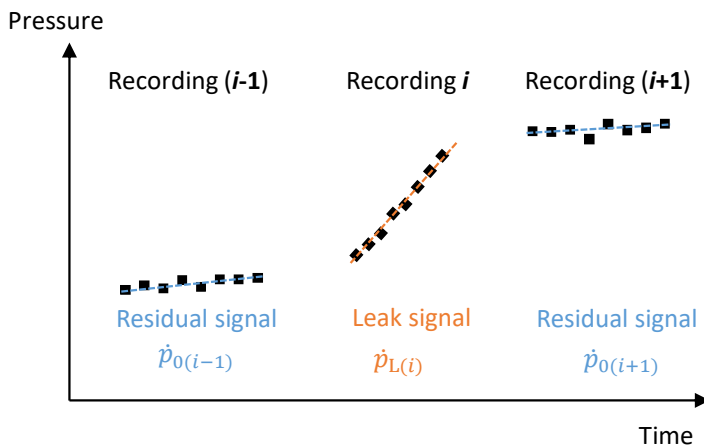


Figure 16. Pressure recording during a leak rate determination

A provisional uncertainty budget is given for each leak rate measurement performed for the comparison, where the measurement repeatability is not taken into account, in Table 3 and Table 4.

**Table 3: Uncertainty budget ( $k = 1$ ) of leak L1 for LNE.**

Leak L1					
300 kPa upstream pressure			700 kPa upstream pressure		
Component	Nominal value	Uncertainty	Component	Nominal value	Uncertainty
$V_m$	71 cm <sup>3</sup>	0.15% · $V_m$	$V_m$	71 cm <sup>3</sup>	0.15% · $V_m$
$\dot{p}_{0i}$	0.005 Pa·s <sup>-1</sup>	0.97% · $\dot{p}_{Li}$	$\dot{p}_{0i}$	0.003 Pa·s <sup>-1</sup>	0.32% · $\dot{p}_{Li}$
$\dot{p}_{Li}$	0.100 Pa·s <sup>-1</sup>	0.17% · $\dot{p}_{Li}$	$\dot{p}_{Li}$	0.500 Pa·s <sup>-1</sup>	0.15% · $\dot{p}_{Li}$
$T_{FM}$	293 K	0.034% · $T_{FM}$	$T_{FM}$	293 K	0.034% · $T_{FM}$
$q$	$2.7 \times 10^{-9}$ mol·s <sup>-1</sup>	1.0% · $q$	$q$	$1.5 \times 10^{-8}$ mol·s <sup>-1</sup>	0.39% · $q$

**Table 4: Uncertainty budget ( $k = 1$ ) of leak L2 for LNE.**

Leak L2					
250 kPa upstream pressure			700 kPa upstream pressure		
Component	Nominal value	Uncertainty	Component	Nominal value	Uncertainty
$V_m$	230 cm <sup>3</sup>	0.12% · $V_m$	$V_m$	230 cm <sup>3</sup>	0.15% · $V_m$
$\dot{p}_{0i}$	0.01 Pa·s <sup>-1</sup>	0.26% · $\dot{p}_{Li}$	$\dot{p}_{0i}$	0.02 Pa·s <sup>-1</sup>	0.033% · $\dot{p}_{Li}$
$\dot{p}_{Li}$	3 Pa·s <sup>-1</sup>	0.026% · $\dot{p}_{Li}$	$\dot{p}_{Li}$	11 Pa·s <sup>-1</sup>	0.025% · $\dot{p}_{Li}$
$T_{FM}$	293 K	0.034% · $T_{FM}$	$T_{FM}$	293 K	0.034% · $T_{FM}$
$q$	$2.5 \times 10^{-7}$ mol·s <sup>-1</sup>	0.29% · $q$	$q$	$1.0 \times 10^{-6}$ mol·s <sup>-1</sup>	0.16% · $q$

### 3.4 UL - Slovenia

The LMPS gas flow primary standard is of volumetric type with a constant volume, usually abbreviated as pVTt (pressure, volume, temperature and time). The system is schematically presented in Figure 17. During a measurement cycle, the hydrogen enters a known and a fixed measuring volume  $V_{mea}$ , resulting in a density change during an observed collection time  $t_{col}$ . The hydrogen densities within the measuring volume at the beginning and end of this time are denoted as  $\rho_1$  and  $\rho_2$  respectively. The basic measurement model for the measured mass flow rate  $q_m$  and the molar flow rate  $q$  is expressed as:

$$q_m = \frac{V_{mea}}{t_{col}} (\rho_2 - \rho_1), \quad q = \frac{q_m}{M} \quad (16)$$

where  $M$  is the molar mass of hydrogen.

The system employs a flying start-stop measurement method and uses a diverter, in the form of a three-way valve with two end-position signals to direct a stable gas flow into or out of the measuring volume. The total collection time is considered as the sum of the measured time recorded for each measurement and the constant correction time, accounting for systematic errors associated with valve switching [6].

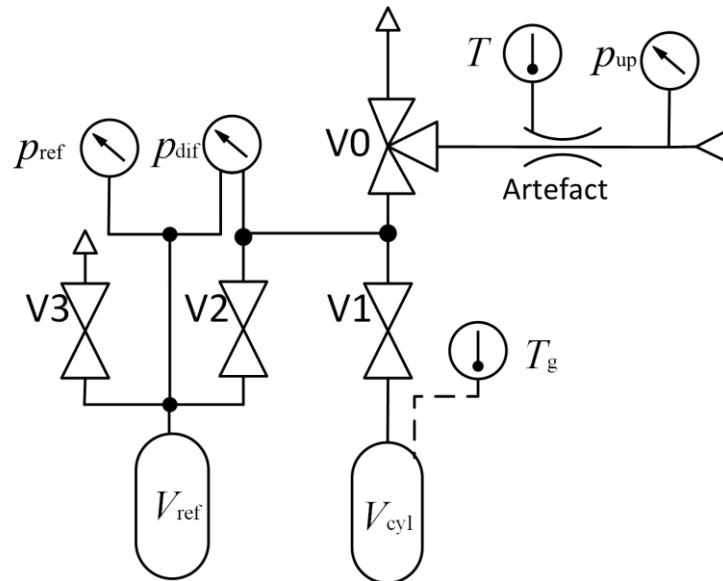


**Figure 17. The scheme of the pVTt system and the artefact**

The majority of the measuring volume  $V_{mea}$  is represented by a calibrated cylinder. The volume of the cylinder  $V_{cyl}$  was determined through the dimensional measurement. A valve was installed directly at the inlet of the cylinder, and the internal volume of the valve and the connecting tube was determined gravimetrically. The volume of the remaining connecting tubes and valves was determined using a gas expansion method. The sum of these three volumes represents the total measuring volume, which is approximately 100 cm<sup>3</sup>.

The temperature of the hydrogen  $T_g$  is measured indirectly using a Pt100 temperature probe embedded in the cylinder wall. To ensure temperature stability, most of the measuring system is immersed in a thermally stabilized water bath. The hydrogen pressure is determined using two digital pressure transducers and an additional reference volume, that is closed during a measurement cycle. The absolute pressure transducer measures a stable reference pressure  $p_{ref}$  within the reference volume (close to the ambient pressure), while the differential pressure transducer measures the time-varying differential pressure  $p_{dif}$  between the measuring volume and the reference volume (up to 2.5 kPa) [7]. The hydrogen density within the measuring volume based on the known gas composition and the measured temperature and pressure is determined using a REFPROP database [5].

The entire measuring system is operated via a real-time controller equipped with dedicated modules for Pt100 temperature measurement, digital inputs and outputs, and digital communication. System monitoring and data acquisition are performed using a personal computer connected within the same local network.

The leak artefact was connected in series with the primary standard system at the inlet of the diverter as presented in Figure 1. Figure 2 shows a photo of the leak connected to the pVTt system. A hand-operated pressure regulator was used to adjust the artefact's inlet pressure  $p_{up}$ , which was monitored by an additional pressure transducer. The outlet pressure of the artefact  $p_{down}$  was equal as the absolute pressure within the measuring volume of the primary standard. Given the approximately linear variation of the outlet pressure during the measurement (due to rise of pressure in the measuring volume up to 2.5 kPa), the reported outlet pressure of the artefact corresponded to the average value of the initial and final pressure. A surface-mounted Pt100 probe was used to measure the temperature of the artefact  $T$ . An additional Pt100 probe was used to measure the ambient temperature. All measurement data was collected and stored on a personal computer for later analysis.

The uncertainty budget of the measured flow rate includes five main contributions. The relative standard uncertainty of the density change  $u(\rho)$ , ranging from 0.056% to 0.059%, accounts for correlated uncertainties in the initial and final values of temperature and reference pressure as well as uncorrelated uncertainties from the differential pressure measurements. The volume standard uncertainty  $u(V_{mea})$ , which is estimated at 0.146%, results from a combination of the dimensional, gravimetric, and gas expansion methods used to characterise all components of the measuring volume, with the gas expansion method having the largest

influence. Smaller contributions come from the uncertainty of the time measurement  $u(t_{cal}) = 0.003\% - 0.017\%$  and the leakage flow  $u(q_{leak}) = 0.003\% - 0.013\%$ . Due to variations in the outlet pressure of the artefact during a single measurement, the resulting change in flow rate introduces an additional uncertainty component  $u(DUT) = 0.041\% - 0.138\%$ . The total combined relative standard uncertainty of the flow rate is therefore equal to  $u(q) = 0.16\% - 0.21\%$ .

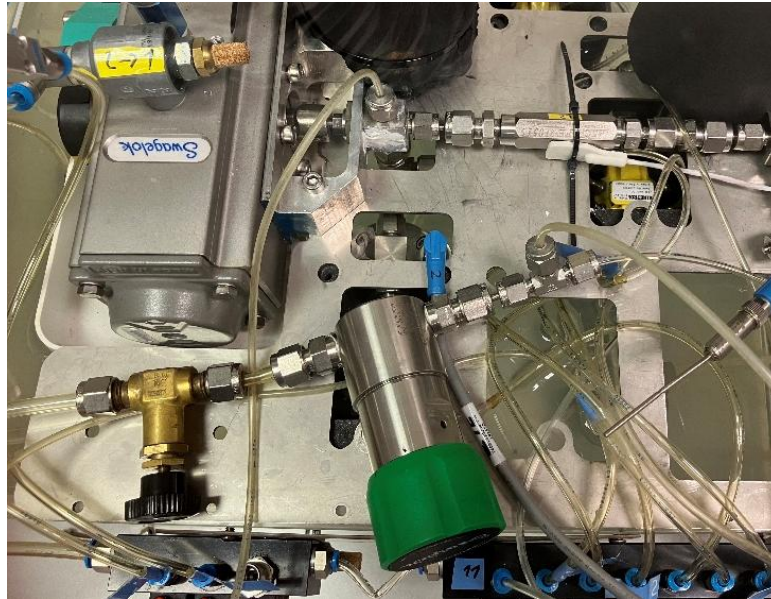


Figure 18. The leak artefact connected in series with the primary standard system

## 4 Characterisation of the transfer standards

The flow rate delivered by a leak artefact is a function of the applied upstream pressure  $p_{up}$ , the downstream pressure  $p_{dw}$  to where the gas flows, the artefact temperature  $T$  and the time of calibration. For these parameters except  $t_{cal}$ , we fixed a nominal value for the comparison respectively that are given in Table 5. The pilot laboratory studied for L1 and L2 the sensitivity of the above-mentioned parameters around their nominal values as well as the stability of the transfer standards over time. In addition, the pilot laboratory determined the internal volume of each leak artefact.

Table 5: Nominal parameters and associated tolerance range for the comparison

Parameter	Nominal value – tolerance range
Upstream pressure $p_{up}$	See Table 1 for values, tolerance $\pm 2\%$
Downstream pressure $p_{dw}$	$p_{dw0} = 100$ kPa, tolerance $\pm 5$ kPa
Temperature $T$	$T_0 = 20$ °C, tolerance $\pm 5$ °C

### 4.1 Sensitivity to the upstream pressure

L1 and L2 were calibrated at five different upstream pressure of hydrogen to determine a polynomial function between the molar flow rate and the upstream pressure  $p_{up}$  when the leak temperature is  $T_0$  and its downstream pressure is  $p_{dw0}$ . We can thus determine a local sensitivity  $\alpha_p(p_{up0})$  of the flow rate at the upstream pressure  $p_{up0}$ . We have:

$$\frac{q(p_{up})}{q(p_{up0})} = 1 + \alpha_p(p_{up0}) \cdot (p_{up} - p_{up0}). \quad (17)$$

Finally:

$$q(p_{up0}) = \frac{q(p_{up})}{1 + \alpha_p(p_{up0}) \cdot (p_{up} - p_{up0})} = C_{pup} \cdot q(p_{up}), \quad (18)$$

where  $C_{pup}$  is upstream pressure temperature coefficient.

Local sensitivity values  $\alpha_p(p_{up0})$  are given for each upstream pressure of each leak in Table 6 and Table 7. The uncertainty of this sensitivity is considered negligible:  $u[\alpha_p(p_{up0})]=0$ .

**Table 6: Flow rate sensitivity to upstream pressure for L1.**

Upstream pressure kPa	Sensitivity kPa <sup>-1</sup>
300	0.74%
700	0.28%

**Table 7: Flow rate sensitivity to upstream pressure for L2.**

Upstream pressure kPa	Sensitivity kPa <sup>-1</sup>
250	0.84%
500	0.37%

## 4.2 Sensitivity to the downstream pressure

The flow from a leak is proportional to the difference of the squares of the pressures upstream and downstream [8],  $p_{up0}$  and  $p_{dw}$ . For given similar downstream pressures  $p_{dw}$  and  $p_{dw0}$ , we then have:

$$q(p_{dw}) = A \cdot (p_{up0}^2 - p_{dw}^2), \quad (19)$$

and

$$q(p_{dw0}) = A \cdot (p_{up0}^2 - p_{dw0}^2), \quad (20)$$

A being a same constant value. In these conditions, it is possible to normalize the measurement of the flow rate  $q$  performed at the downstream pressure  $p_{dw}$  to the flow rate, which would have been for  $p_{dw0} = 100$  kPa. From (19) and (20), we get:

$$q(p_{dw0}) = q(p_{dw}) \cdot \frac{p_{up0}^2 - p_{dw0}^2}{p_{up0}^2 - p_{dw}^2} = C_{pdw} \cdot q(p_{dw}), \quad (21)$$

Where  $C_{pdw}$  is the downstream pressure correction coefficient.

## 4.3 Sensitivity to the temperature

It is well known that gas flow rates through leak elements are sensitive to temperature to a certain extent depending on the nature of the element [9]. For physical leak elements (case of L1 and L2), the temperature coefficient  $\alpha_T(T_0)$  for the temperature  $T_0$ , is usually lower than  $0.5 \% \cdot K^{-1}$ . Under the same upstream and downstream pressures, the ratio between the flow rate at the temperature  $T$  and the flow rate at the temperature  $T_0$  can be written:

$$\frac{q(T)}{q(T_0)} = 1 + \alpha_T(T_0) \cdot (T - T_0), \quad (22)$$

which leads to:

$$q(T_0) = \frac{q(T)}{1 + \alpha_T(T_0) \cdot (T - T_0)} = C_T \cdot q(T), \quad (23)$$

where  $C_T$  is the temperature correction coefficient.

The temperature coefficient was determined experimentally for L1 and L2 at  $T_0 = 20\text{ °C}$ . Molar flow rates were measured for fixed upstream and downstream pressures at nominal temperatures of  $15\text{ °C}$ ,  $20\text{ °C}$  and  $25\text{ °C}$ . The calculation of the slope of the linear regression of the function  $\frac{q(T)}{q(T_0)} - 1 = f(T - T_0)$  leads to the temperature coefficient  $\alpha_T(T_0)$ . A graphic representation of measurements performed for the leak L2 is shown Figure 19.

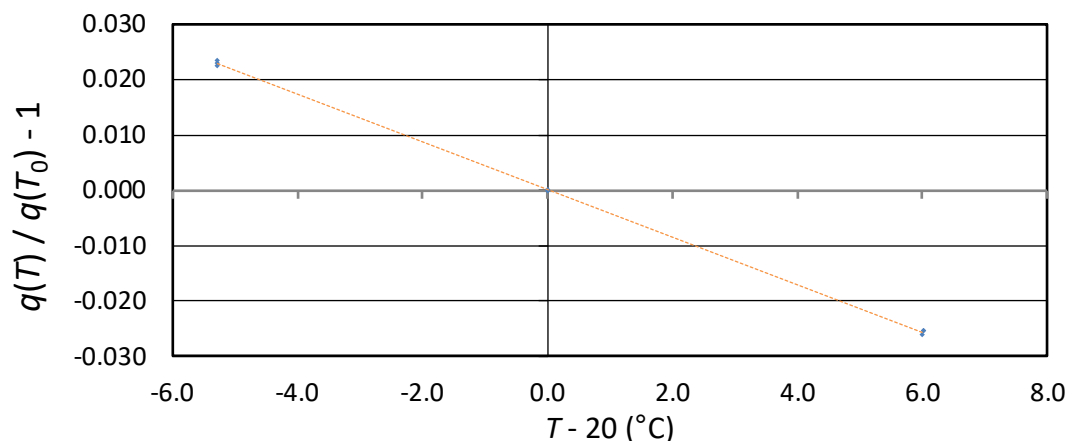


**Figure 19. Relative flow measurement variation at different temperatures around  $20\text{ °C}$  for the leak L2.**

The temperature coefficient  $\alpha_T(T_0)$  of each leak with its uncertainty is given in Table 8 for leak L1 and in Table 9 for leak L2. The upstream pressure was set to a value allowing a sufficient repeatability of the measurements. It is also indicated in the Tables.

**Table 8: Temperature coefficient of L1.**

Upstream pressure kPa	Temperature coefficient $\text{K}^{-1}$	Uncertainty (k=1) $\text{K}^{-1}$
700	-0.51%	0.050%

**Table 9: Temperature coefficient of L2.**

Upstream pressure kPa	Temperature coefficient $\text{K}^{-1}$	Uncertainty (k=1) $\text{K}^{-1}$
500	-0.43%	0.050%

#### 4.4 Stability over time

The main issue of a transfer standard is usually its stability over the duration of the comparison. The stability of L1 and L2 was assessed by successive calibrations between measurements of the participants. For its more accurate assessment, calibrations were performed with a leak downstream pressure equivalent to vacuum. It is assumed that the relative drift of the flow rate would be similar at atmospheric downstream pressure. The leak temperature standard uncertainty is estimated to be  $0.1\text{ °C}$ . With a nominal temperature coefficient of  $0.5\% \cdot \text{K}^{-1}$ , the relative standard uncertainty for the stability check is 0.05%. The measurement repeatability was in all cases lower than 0.01% which can thus be neglected compared to the uncertainty due to the temperature.

The successive drift checking are listed in Table 10 and Table 11 for L1 and L2 respectively. The final checking of L2 could not have been performed due to a late calibration by the last participant (see section 5).

**Table 10: Flow rate stability of L1.**

Date (day/month/year)	Relative drift
20/12/2024	-
25/03/2025	-0.79%
17/06/2025	-2.24%

**Table 11: Flow rate stability of L2.**

Date (day/month/year)	Relative drift
15/01/2025	-
09/04/2025	-0.12%

The uncertainty  $u_{stab}$  due to the stability of the transfer standard is estimated using the maximum drift considering an associated rectangular distribution, that leads to the values listed in Table 12.

**Table 12: Standard uncertainty due to the transfer standard stability.**

Transfer standard	Uncertainty of stability
L1	1.3%
L2	0.068%

## 4.5 Internal volume

The internal volumes of the leak artefacts were calibrated and their values were communicated to UL (L2) and CNAM (L1). The calibration was performed in the connexion configuration used, *i.e.* with a VCR adapter for L1 and without an adapter for L2. The experimental setup to achieve internal volume measurements is shown Figure 20.

The flow standard is the LNE former constant-volume flowmeter CVFM1 for leak rates referred to vacuum. The measurement consisted of the calibration of the dead volume  $V_{d,A}$  (Figure 20-A) which comprises the leak internal volume  $V_{int}$  to be determined and the dead volume  $V_d$  of other parts; it has to be noticed that  $V_{int}$  is small compared to  $V_d$ . The leak (L1 or L2) is connected together with an auxiliary capillary leak in a parallel arrangement and both have their upstream pressure regulated with their own pressure controller (not represented). Upstream pressures are adjusted such as the total flow rate ( $q_L + q_{aux,A}$ ) is about  $6 \times 10^{-4} \text{ Pa} \cdot \text{m}^3 \cdot \text{s}^{-1}$ . The procedure is similar to that described in [2], using the general calibration setup of Figure 14.

The determined volume in setup A is:

$$V_{d,A} = V_d + V_{int} + \varepsilon_V, \quad (24)$$

$\varepsilon_V$  being the measurement error of  $V_{d,A}$ .

In setup B (Figure 20-B), the leak under study is replaced by a blank flange and the dead volume  $V_{d,B}$  is determined again in same experimental conditions, in particular the total flow rate  $q_{aux,B}$  has the same value as in setup A.

The determined volume in setup B is:

$$V_{d,B} = V_d + \varepsilon_V, \quad (25)$$

With the same measurement error  $\varepsilon_V$ , since  $V_{d,B} \approx V_{d,A}$ .

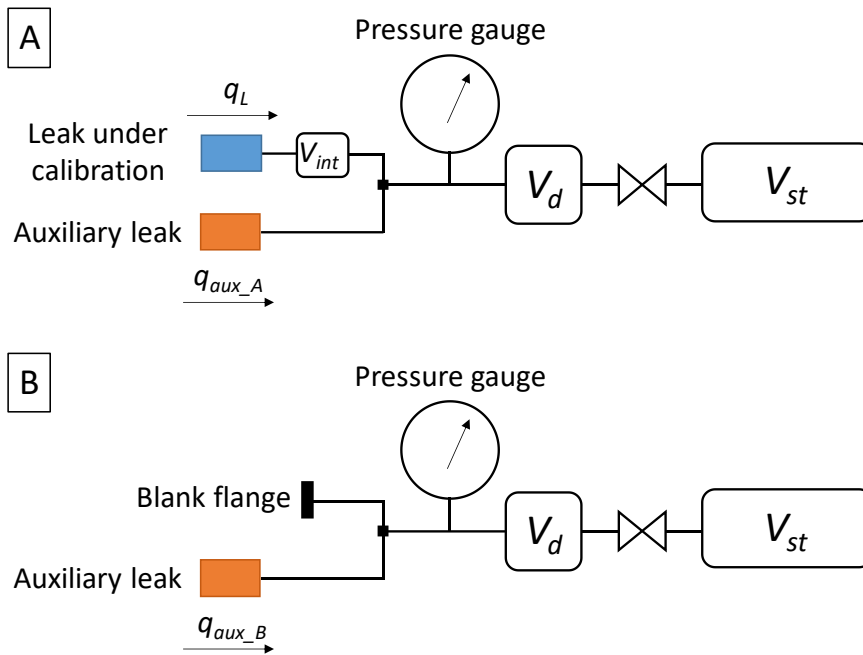


**Figure 20. Two-steps procedure to calibrate the internal volume  $V_{int}$  of the transfer standards.**

Combining equations (24) and (25), we deduce:

$$V_{int} = V_{d\_B} - V_{d\_A} \tag{26}$$

By cancelling the measurement error, this procedure allows one to restrict the uncertainty of  $V_{int}$  to the quadratic mean of the respective measurement repeatability of  $V_{d\_A}$  and  $V_{d\_B}$ . Determined internal volumes of L1 and L2 with their standard uncertainties are presented in Table 13.

**Table 13: Internal volumes of the transfer standard in the configuration connection to the participants' standards.**

Transfer standard (participant)	Internal volume cm <sup>3</sup>	Uncertainty (k=1) cm <sup>3</sup>
L1 (CNAM)	1.726	0.030
L2 (UL)	0.510	0.050

## 5 Schedule of the comparison

Calibration dates of the transfer standards are indicated in Table 14 (L1) and in Table 15 (L2), as they were reported by the participants.

**Table 14: Calibration schedule of L1.**

Date format is "day/month/year"

L1	
Participant	Calibration period
CMI	17/03/2025
LNE	07/04/2025 and 09/04/2025
CNAM	03/06/2025 to 06/06/2025

**Table 15: Calibration schedule of L2.**

Date format is “day/month/year”

L2	
Participant	Calibration period
UL	14/03/2025 to 21/03/2025
LNE	15/04/2025
CMI	08/09/2025

## 6 Calibration procedure for the comparison

The following procedure was distributed and approved by the participants before starting the leak rates comparison.

### 6.1 Quantity to be determined

The results shall be given in moles per second at the temperature of the leak artefact. For that purpose, if the measurand from a given flowmeter is in pressure and volume unit, the conversion to the molar flow rate shall be performed considering the real gas conditions.

### 6.2 General procedure

#### 6.2.1 Temperature

The leak artefacts are characterised at 20 °C, so ideally each participant will perform the calibration at 20 °C. A threshold of 5 °C around 20 °C is permissible. The participants will provide their uncertainty in temperature. The pilot laboratory will apply correction to get the molar flow rate at 20 °C. Regarding the feeble temperature coefficient (around 0,5% per °C), it is **not** required to operate any device for thermalizing the artefact.

#### 6.2.2 Downstream pressure

The downstream pressure is fixed at 100 kPa. A threshold of 5 kPa around 100 kPa is permissible. The participants will provide the downstream pressure value and its uncertainty. The pilot Laboratory will apply correction to get the molar flow rate for a downstream pressure of 100 kPa.

#### 6.2.3 Upstream pressure

The upstream pressure shall be as close as possible of the nominal required pressures (Table 6 and Table 7). The participants will provide the upstream pressure value and its uncertainty. The pilot laboratory will apply correction to get the molar flow rate for the nominal upstream pressures.

#### 6.2.4 Number of measurements

Three measurements are required within the shortest time possible in order to stay in repeatability conditions.

#### 6.2.5 Summarised operating mode

For a leak calibration:

- 1- Connect the leak to the flow standard.
- 2- Connect the device for generating the upstream pressure.
- 3- Attach a temperature sensor on the body of the leak artefact.
- 4- Apply one of the two hydrogen upstream pressure.
- 5- Perform three measurements within the shortest time possible
- 6- Apply the second hydrogen upstream pressure (if the flow rate is in the range of the flow standard).
- 7- Perform three measurements within the shortest time possible.
- 8- Dismount the leak artefact from the calibration setup.

## 7 Comparison results

### 7.1 Set of measurements

An Excel sheet was distributed to the participants to report their calibration data, shown Figure 21.

Notations used									
p <sub>up</sub>	Applied upstream pressure and its standard uncertainty $u(p_{up})$								
p <sub>dw</sub>	Downstream pressure and its standard uncertainty $u(p_{dw})$								
T	Measured leak temperature and its standard uncertainty $u(T)$								
$q(p_{up}; p_{dw}; T)$	Measured molar flow rate and its standard uncertainty $u(q)$								
T <sub>room</sub>	Room temperature during the calibration								
Laboratory name									
Date									
T <sub>room</sub> (°C)									
Leak L1									
p <sub>up</sub> nominal	Measurement number	p <sub>up</sub>	u(p <sub>up</sub> )	p <sub>dw</sub>	u(p <sub>dw</sub> )	T	u(T)	$q(p_{up}; p_{dw}; T)$	u(q)
kPa		kPa	kPa	kPa	kPa	°C	°C	mol·s <sup>-1</sup>	mol·s <sup>-1</sup>
700	1								
	2								
	3								
300	1								
	2								
	3								

**Figure 21. Picture of the Excel sheet in which the calibration data shall be reported.**

It allows the pilot laboratory to calculate reduced results for a comparison at the same conditions of upstream and downstream pressure and temperature.

### 7.2 Reducing the results

The flow rates  $q(p_{up}; p_{dw}; T)$  measured by the participants are reduced to  $q(p_{up0}; p_{dw0}; T_0)$  with  $T_0 = 20$  °C,  $p_{dw0} = 100$  kPa and  $p_{up0}$  corresponding to the required flow rates (see Transfer standards details. Table 1), using equations (18), (21) and (23):

$$q_{comp} = C_{pup} \cdot C_{pdw} \cdot C_T \cdot q(p_{up}; p_{dw}; T). \quad (27)$$

The uncertainty of the reduced flow rate is thus:

$$\frac{u[q(p_{up0}; p_{dw0}; T_0)]}{q(p_{up0}; p_{dw0}; T_0)} = \left[ \left[ \frac{u(C_{pup})}{C_{pup}} \right]^2 + \left[ \frac{u(C_{pdw})}{C_{pdw}} \right]^2 + \left[ \frac{u(C_T)}{C_T} \right]^2 + \left[ \frac{u[q(p_{up}; p_{dw}; T)]}{q(p_{up}; p_{dw}; T)} \right]^2 \right]^{1/2} \cdot \left[ \frac{u_{rep}}{q(p_{up}; p_{dw}; T)} \right]^2 \quad (28)$$

The uncertainty of the flow rate  $u[q(p_{up}; p_{dw}; T)]$  is given by the participant and the repeatability  $u_{rep}$  is calculated by the pilot laboratory. It is estimated using the experimental standard deviation of the three flow measurements performed.

The uncertainty of the correction coefficients  $C_T$ ,  $C_{pup}$  and  $C_{pdw}$  are calculated by means of the variance propagation laws considering that the variables are independent. It leads to the expressions below:

$$[u(C_T)]^2 = \frac{[\alpha_T(T_0)]^2}{[1 + \alpha_T(T_0)(T - T_0)]^4} [u(T)]^2 + \left[ \frac{T - T_0}{1 + \alpha_T(T_0)} \right]^2 [u(\alpha_T(T_0))]^2. \quad (29)$$

The uncertainty  $u(T)$  is given by the participant and the uncertainty  $u(\alpha_T(T_0))$  is that of Table 8 and Table 9.

$$[u(C_{pup})]^2 = \frac{[\alpha_p(T_0)]^2}{[1+\alpha_p(p_{up0}) \cdot (p_{up}-p_{up0})]^4} [u(p_{up})]^2 + \left[ \frac{p_{up}-p_{up0}}{1+\alpha_p(p_{up0})} \right]^2 [u(\alpha_p(p_{up0}))]^2, \quad (30)$$

with  $\alpha_p(p_{up0}) = 0$  and the uncertainty ( $p_{up}$ ) is given by the participant.

$$[u(C_{pdw})]^2 = \frac{[2p_{dw}(p_{up0}^2 - p_{dw0}^2)]^2}{(p_{up0}^2 - p_{dw0}^2)^4} [u(p_{dw})]^2. \quad (31)$$

The uncertainty  $u(p_{dw})$  is given by the participants.

To assess the uncertainty of the comparison  $q_{comp}$ , we take into account the stability of the transfer standard over the course of the comparison combining quadratically the uncertainty  $u_{stab}$  (section 4.4) with  $u[q(p_{up0}; p_{dw0}; T_0)]$ :

$$u(q_{comp}) = \left[ [u[q(p_{up0}; p_{dw0}; T_0)]]^2 + [u_{stab}]^2 \right]^{\frac{1}{2}}. \quad (32)$$

The presented results in sections 7.3 and 7.4 are reduced results for each leak calibration. One can find in the annex the raw results provided by the participants and intermediate calculations of the correction coefficients  $C_T$ ,  $C_{pup}$  and  $C_{pdw}$  with their correspondent uncertainty. A results table contains for each participant the calibration date, the measured flow rate  $q_{comp}$  with its relative enlarged uncertainty, and the measurement repeatability expressed relatively

### 7.3 Results for L1

Calibration results for the upstream pressures 300 kPa and 700 kPa are respectively given in Table 16 and Table 17 and shown Figure 22.

**Table 16: Calibration results of the leak L1 at 300 kPa.**

Date format is “day/month/year”

L1 - Calibration at $p_{up} = 300$ kPa				
Laboratory	Date	$q_{comp}$ mol·s <sup>-1</sup>	$u_{rep}/q_{comp}$	$U(q_{comp})/q_{comp}$ ( $k = 2$ )
CMI	17/03/2025	2.712E-9	4.8%	13%
CNAM	06/06/2025	3.423E-9	1.7%	5.0%
LNE	09/04/2025	2.749E-9	0.51%	3.8%

**Table 17: Calibration results of the leak L1 at 700 kPa.**

Date format is “day/month/year”

L1 - Calibration at $p_{up} = 700$ kPa				
Laboratory	Date	$q_{comp}$ mol·s <sup>-1</sup>	$u_{rep}/q_{comp}$	$U(q_{comp})/q_{comp}$ ( $k = 2$ )
CMI	17/03/2025	1.602E-8	0.45%	4.4%
CNAM	03/06/2025	1.886E-8	1.1%	4.3%
LNE	07/04/2025	1.546E-8	0.59%	3.3%

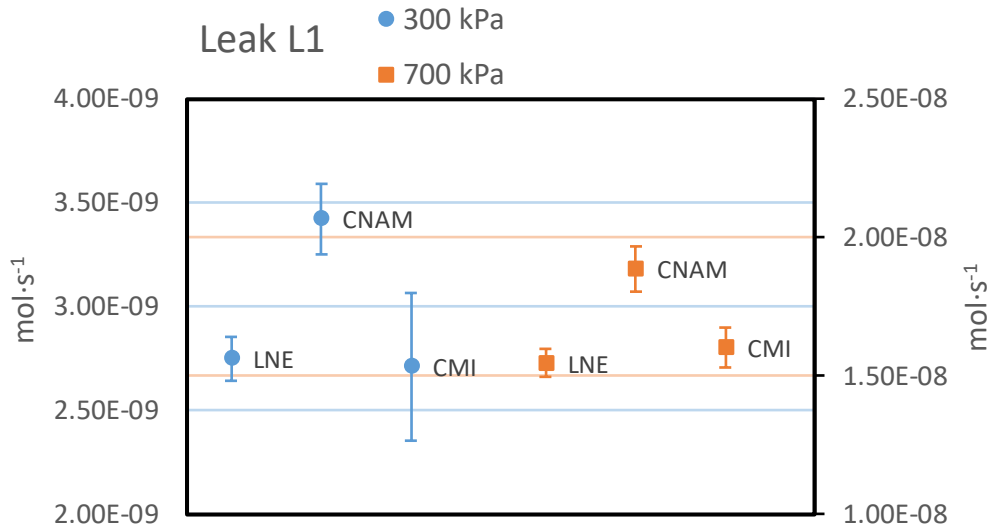


Figure 22. Calibration results of the leak L1 for respective upstream pressures of 300 kPa and 700 kPa.

**Vertical bars are enlarged uncertainties**

In this range of comparison, participants have similar calibration uncertainty except for CMI at  $5.5 \times 10^{-7} \text{ mol}\cdot\text{s}^{-1}$  due to a high repeatability uncertainty. Results of CMI and LNE are compatible within their calibration uncertainty.

CNAM calibrated are not compatible within the uncertainty, with neither CMI nor LNE. One can notice a calibrated value for CNAM systematically higher by 20% than that of LNE.

**7.4 Results for L2**

Calibration results for the upstream pressures 250 kPa and 500 kPa are respectively given in Table 18 and Table 19 and shown Figure 22 and Figure 23.

Table 18: Calibration results of the leak L2 at 250 kPa.

Date format is “day/month/year”

L2 - Calibration at $p_{up} = 250 \text{ kPa}$				
Laboratory	Date	$q_{comp}$ mol·s <sup>-1</sup>	$u_{rep}/q_{comp}$	$U(q_{comp})/q_{comp}$ ( $k = 2$ )
CMI	08/09/2025	2.438E-7	0.53%	1.4%
LNE	15/04/2025	2.614E-7	0.060%	0.70%
UL	21/03/2025	2.558E-7	0.14%	0.57%

Table 19: Calibration results of the leak L2 at 500 kPa.

Date format is “day/month/year”

L2 - Calibration at $p_{up} = 500 \text{ kPa}$				
Laboratory	Date	$q_{comp}$ mol·s <sup>-1</sup>	$u_{rep}/q_{comp}$	$U(q_{comp})/q_{comp}$ ( $k = 2$ )
CMI	08/09/2025	9.618E-7	0.20%	1.0%
LNE	15/04/2025	9.922E-7	0.015%	0.34%
UL	21/03/2025	9.869E-7	0.011%	0.42%

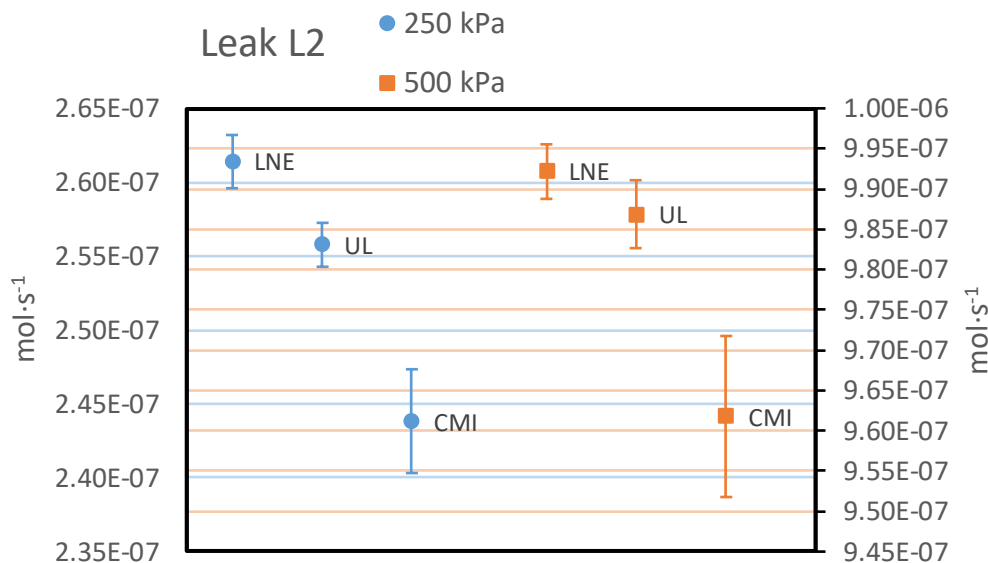


**Figure 23. Calibration results of the leak L2 for respective upstream pressures of 250 kPa and 500 kPa.**

**Vertical bars are enlarged uncertainties**

In this comparison flow range LNE results are higher than those of UL by a constant value of about  $5.5 \times 10^{-7} \text{ mol} \cdot \text{s}^{-1}$ . LNE and UL results are compatible within the calibration uncertainty for the highest flow rate of  $9.9 \times 10^{-7} \text{ mol} \cdot \text{s}^{-1}$ . CMI results are systematically lower than those of LNE and UL by about 5% for the rate of  $5.5 \times 10^{-7} \text{ mol} \cdot \text{s}^{-1}$  and about 3% for the rate of  $9.9 \times 10^{-7} \text{ mol} \cdot \text{s}^{-1}$ .

## 8 Conclusion

Comparison of small leaks flowing at atmosphere remains challenging. The satisfactory stability of the transfer standards with a relative uncertainty contribution lower than 1.5% cannot justify deviations between some of the measurements. Comparison results of CMI and LNE are compatible for the smaller flow rates for the highest flow rate of hydrogen at  $9.9 \times 10^{-7} \text{ mol} \cdot \text{s}^{-1}$ , between LNE and UL. Participant laboratories identified potential sources for such discrepancies: leakage in the measurement system (LNE), limitations of the PVTt system to keep the downstream pressure constant (UL), leak in the system, or/and to poor knowledge of the  $A_R$  and  $B_R$  coefficients of hydrogen (CNAM).

Flow measurement systems need to be further investigated at the light of those preliminary results.

## References

- [1] Kragh, H. "The Lorenz-Lorentz Formula: Origin and Early History." *Substantia*, 2(2), 2018, 7–18. <https://doi.org/10.13128/Substantia-56>.
- [2] F. Boineau, M. D. Plimmer and E. Mahé, "Volume calibration using a comparison method with a transfer leak flow rate", *ACTA IMEKO*, vol. 9, n° 5, Art. n° 5, déc. 2020, doi: [10.21014/acta\\_imeko.v9i5.997](https://doi.org/10.21014/acta_imeko.v9i5.997).
- [3] F. Boineau and M. D. Plimmer, "A technique to improve low leak rate measurement with a constant-volume flowmeter", in *Proceedings of the 6th IMEKO TC16 Conference on Pressure and Vacuum Measurement*, Cavtat-Dubrovnik, CROATIA: IMEKO, 2023, p. 1-5. doi: [10.21014/tc16-2022.120](https://doi.org/10.21014/tc16-2022.120).

- 
- [4] P. J. Mohr, D. B. Newell, B. N. Taylor, et E. Tiesinga, « Data and analysis for the CODATA 2017 special fundamental constants adjustment\* », *Metrologia*, vol. 55, n° 1, p. 125, janv. 2018, doi: 10.1088/1681-7575/aa99bc
- [5] Lemmon, E.W., Bell, I.H., Huber, M.L., McLinden, M.O. NIST Standard Reference Database 23: Reference Fluid Thermodynamic and Transport Properties-REFPROP, Version 10.0, National Institute of Standards and Technology, Standard Reference Data Program, Gaithersburg, 2018.
- [6] Žibret, P.; Bobovnik, G.; Kutin, J. "Time-Correction Model Based on Diverter Speed for a pVTt Gas Flow Primary Standard." *Sensors* 2022, 22, 4001. <https://doi.org/10.3390/s22114001>.
- [7] Žibret, P., Bobovnik, G., Kutin, J. "Correction for the Temperature effects in a pVTt Gas Flow Primary Standard Employing a Dynamic Method." *Measurement*, 207, 2022, 112375. <https://doi.org/10.1016/j.measurement.2022.112375>.
- [8] P.G. Spazzini, G. La Piana, A. Piccato, V. Delnegro, M. Viola "Flow leaks normalization", *Measurement*, 221, 2023, 113429. <https://doi.org/10.1016/j.measurement.2023.113429>
- [9] C. D. Ehrlich et J. A. Basford, "Recommended practices for the calibration and use of leaks ", *Journal of Vacuum Science & Technology A*, vol. 10, no 1, p. 1 17, 1992, doi: 10.1116/1.578137.

## Annex: Reported data of the participating laboratories and intermediate calculations

### Notations used in the Tables

$p_{dw}$	Downstream pressure and its standard uncertainty $u(p_{dw})$
$p_{up}$	Applied upstream pressure and its standard uncertainty $u(p_{up})$
$T$	Measured leak artefact temperature and its standard uncertainty $u(T)$
$q(p_{up}; p_{dw}; T)$	Measured molar flow rate and its standard uncertainty $u(q)$
$C_T$	Calculated temperature correction coefficient and its relative standard uncertainty $ur(C_T)$
$C_{p_{dw}}$	Calculated downstream pressure correction coefficient and its relative standard uncertainty $ur(p_{dw})$
$C_{p_{up}}$	Calculated upstream pressure correction coefficient and its relative standard uncertainty $ur(p_{up})$
$q_{comp}$	Calculated flow rate in the nominal conditions of the comparison and its relative standard uncertainty $ur(q_{comp})$

### Leak L1, CMI

Leak L1											
$p_{up}$ nominal	Measurement number	Date	$p_{up}$	$u(p_{up})$	$p_{dw}$	$u(p_{dw})$	$T$	$u(T)$	$q(p_{up}; p_{dw}; T)$	$u(q)$	
kPa			kPa	kPa	kPa	kPa	°C	°C	mol·s <sup>-1</sup>	mol·s <sup>-1</sup>	
300	1	17/03/2025	303.16	0.030	97.99	0.012	23.02	0.16	2.890E-09	1.4E-10	
	2	17/03/2025	300.81	0.030	98.73	0.012	23.03	0.16	2.670E-09	9.8E-11	
	3	17/03/2025	299.76	0.030	98.73	0.012	23.01	0.16	2.560E-09	1.0E-10	
700	1	17/03/2025	700.02	0.070	96.52	0.012	23.35	0.16	1.580E-08	2.6E-10	
	2	17/03/2025	702.05	0.070	97.59	0.012	23.09	0.16	1.592E-08	2.5E-10	
	3	17/03/2025	700.69	0.070	97.63	0.012	23.07	0.16	1.573E-08	2.3E-10	

### L1 – 300 kPa

$C_T$	$C_{p_{dw}}$	$C_{p_{up}}$	$q_{comp}$	$u(T)$	$u(p_{dw})$	$u(p_{up})$	$u(q)$	$ur(q)$	$ur(C_T)$	$ur(C_{p_{dw}})$	$ur(C_{p_{up}})$	$ur_{rep}$	$ur(q_{comp})$
			mol/s	°C	kPa	kPa	mol/s						
1.0156	0.9952	0.97703	2.854E-09	0.160	0.012	0.030	1.4E-10	5.2E-02	1.7E-03	3.0E-05	2.1E-04	4.8E-02	7.2E-02
1.0157	0.9969	0.99401	2.687E-09	0.160	0.012	0.030	9.8E-11	3.6E-02	1.7E-03	3.0E-05	2.2E-04	4.8E-02	6.2E-02
1.0155	0.9968	1.00182	2.596E-09	0.160	0.012	0.030	1.0E-10	3.7E-02	1.7E-03	3.0E-05	2.2E-04	4.8E-02	6.3E-02

### L1 – 700 kPa

$C_T$	$C_{p_{dw}}$	$C_{p_{up}}$	$q_{comp}$	$u(T)$	$u(p_{dw})$	$u(p_{up})$	$u(q)$	$ur(q)$	$ur(C_T)$	$ur(C_{p_{dw}})$	$ur(C_{p_{up}})$	$ur_{rep}$	$ur(q_{comp})$
			mol/s	°C	kPa	kPa	mol/s						
1.0173	0.9986	0.99996	1.605E-08	0.160	0.012	0.070	2.6E-10	1.6E-02	2.5E-03	4.8E-06	2.0E-04	4.5E-03	2.3E-02
1.0160	0.9990	0.99426	1.607E-08	0.160	0.012	0.070	2.5E-10	1.6E-02	2.4E-03	4.9E-06	1.9E-04	4.5E-03	2.2E-02
1.0159	0.9990	0.99807	1.593E-08	0.160	0.012	0.070	2.3E-10	1.4E-02	2.4E-03	4.9E-06	2.0E-04	4.5E-03	2.1E-02

### Leak L1, CNAM

Laboratory name	CNAM												
$T_{room}$ (°C)	25°C +/- 1°C												

Leak L1											
$p_{up}$ nominal	Measurement number	Date	$p_{up}$	$u(p_{up})$	$p_{dw}$	$u(p_{dw})$	$T$	$u(T)$	$q(p_{up}; p_{dw}; T)$	$u(q)$	
kPa			kPa	kPa	kPa	kPa	°C	°C	mol·s <sup>-1</sup>	mol·s <sup>-1</sup>	
300	1	06/06/2025	300.00	0.20	100.32	0.10	23.54	0.40	3.421E-09	3.4E-11	
	2	06/06/2025	300.00	0.20	100.33	0.10	24.63	0.40	3.293E-09	3.3E-11	
	3	06/06/2025	300.00	0.20	100.35	0.10	24.70	0.40	3.323E-09	3.3E-11	
700	1	03/06/2025	700.00	0.20	100.99	0.10	24.93	0.40	1.849E-08	1.8E-10	
	2	03/06/2025	700.00	0.20	100.90	0.10	25.01	0.40	1.813E-08	1.8E-10	
	3	03/06/2025	700.00	0.20	100.95	0.10	25.06	0.40	1.849E-08	1.8E-10	

### L1 – 300 kPa

$C_T$	$C_{p_{dw}}$	$C_{p_{up}}$	$q_{comp}$	$u(T)$	$u(p_{dw})$	$u(p_{up})$	$u(q)$	$ur(q)$	$ur(C_T)$	$ur(C_{p_{dw}})$	$ur(C_{p_{up}})$	$ur_{rep}$	$ur(q_{comp})$
			mol/s	°C	kPa	kPa	mol/s						
1.0184	1.0008	1.00000	3.487E-09	0.400	0.100	0.200	3.4E-11	1.0E-02	2.7E-03	2.5E-04	1.5E-03	1.7E-02	2.5E-02
1.0242	1.0008	1.00000	3.375E-09	0.400	0.100	0.200	3.3E-11	9.6E-03	3.1E-03	2.5E-04	1.5E-03	1.7E-02	2.5E-02
1.0245	1.0009	1.00000	3.407E-09	0.400	0.100	0.200	3.3E-11	9.7E-03	3.1E-03	2.5E-04	1.5E-03	1.7E-02	2.5E-02

## L1 – 700 kPa

$C_T$	$C_{p\_dw}$	$C_{p\_up}$	$q_{comp}$	$u(T)$	$u(p\_dw)$	$u(p\_up)$	$u(q)$	$ur(q)$	$ur(C_T)$	$ur(C_{p\_dw})$	$ur(C_{p\_up})$	$ur_{rep}$	$ur(q_{comp})$
			mol/s	°C	kPa	kPa	mol/s						
1.0258	1.0004	1.00000	1.898E-08	0.400	0.100	0.200	1.8E-10	9.8E-03	4.6E-03	4.2E-05	5.6E-04	1.1E-02	2.2E-02
1.0262	1.0004	1.00000	1.861E-08	0.400	0.100	0.200	1.8E-10	9.6E-03	4.7E-03	4.2E-05	5.6E-04	1.1E-02	2.2E-02
1.0265	1.0004	1.00000	1.899E-08	0.400	0.100	0.200	1.8E-10	9.8E-03	4.7E-03	4.2E-05	5.6E-04	1.1E-02	2.2E-02

## Leak L1, LNE

Laboratory name	LNE												
$T_{room}$ (°C)	20 °C ± 1°C												

Leak L1											
$p_{up}$ nominal	Measurement number	Date	$p_{up}$	$u(p_{up})$	$p_{dw}$	$u(p_{dw})$	$T$	$u(T)$	$q(p_{up}; p_{dw}; T)$	$u(q)$	
kPa			kPa	kPa	kPa	kPa	°C	°C	mol·s <sup>-1</sup>	mol·s <sup>-1</sup>	
300	1	09/04/2025	300.00	0.20	100.09	0.01	20.46	0.10	2.726E-09	2.7E-11	
	2	09/04/2025	300.00	0.20	99.95	0.01	20.47	0.10	2.754E-09	2.8E-11	
	3	09/04/2025	300.00	0.20	100.01	0.01	20.48	0.10	2.747E-09	2.7E-11	
700	1	07/04/2025	699.99	0.20	100.02	0.01	20.08	0.10	1.539E-08	6.0E-11	
	2	07/04/2025	699.99	0.20	100.02	0.01	20.04	0.10	1.541E-08	6.0E-11	
	3	07/04/2025	699.99	0.20	100.00	0.01	20.18	0.10	1.555E-08	6.1E-11	

## L1 – 300 kPa

$C_T$	$C_{p\_dw}$	$C_{p\_up}$	$q_{comp}$	$u(T)$	$u(p\_dw)$	$u(p\_up)$	$u(q)$	$ur(q)$	$ur(C_T)$	$ur(C_{p\_dw})$	$ur(C_{p\_up})$	$ur_{rep}$	$ur(q_{comp})$
			mol/s	°C	kPa	kPa	mol/s						
1.0024	1.0002	1.00001	2.733E-09	0.100	0.010	0.200	2.7E-11	9.9E-03	5.6E-04	2.5E-05	1.5E-03	5.1E-03	1.9E-02
1.0024	0.9999	1.00001	2.760E-09	0.100	0.010	0.200	2.8E-11	1.0E-02	5.6E-04	2.5E-05	1.5E-03	5.1E-03	1.9E-02
1.0024	1.0000	1.00001	2.754E-09	0.100	0.010	0.200	2.7E-11	1.0E-02	5.6E-04	2.5E-05	1.5E-03	5.1E-03	1.9E-02

## L1 – 700 kPa

$C_T$	$C_{p\_dw}$	$C_{p\_up}$	$q_{comp}$	$u(T)$	$u(p\_dw)$	$u(p\_up)$	$u(q)$	$ur(q)$	$ur(C_T)$	$ur(C_{p\_dw})$	$ur(C_{p\_up})$	$ur_{rep}$	$ur(q_{comp})$
			mol/s	°C	kPa	kPa	mol/s						
1.0004	1.0000	1.00001	1.540E-08	0.100	0.010	0.200	6.0E-11	3.9E-03	5.5E-04	4.2E-06	5.6E-04	5.9E-03	1.7E-02
1.0002	1.0000	1.00001	1.541E-08	0.100	0.010	0.200	6.0E-11	3.9E-03	5.3E-04	4.2E-06	5.6E-04	5.9E-03	1.7E-02
1.0009	1.0000	1.00001	1.556E-08	0.100	0.010	0.200	6.1E-11	3.9E-03	6.0E-04	4.2E-06	5.6E-04	5.9E-03	1.7E-02

## Leak L2, CMI

## L2 – 250 kPa

$C_T$	$C_{p\_dw}$	$C_{p\_up}$	$q_{comp}$	$u(T)$	$u(p\_dw)$	$u(p\_up)$	$u(q)$	$ur(q)$	$ur(C_T)$	$ur(C_{p\_dw})$	$ur(C_{p\_up})$	$ur_{rep}$	$ur(q_{comp})$
			mol/s	°C	kPa	kPa	mol/s						
1.0144	0.9999	1.00422	2.425E-07	0.160	0.012	0.025	1.0E-09	4.1E-03	1.8E-03	4.6E-05	2.1E-04	5.3E-03	7.0E-03
1.0127	0.9995	0.99408	2.451E-07	0.160	0.012	0.025	1.1E-09	4.5E-03	1.6E-03	4.6E-05	2.1E-04	5.3E-03	7.2E-03
1.0129	0.9995	1.00532	2.439E-07	0.160	0.012	0.025	1.1E-09	4.5E-03	1.6E-03	4.6E-05	2.1E-04	5.3E-03	7.2E-03

## L2 – 500 kPa

$C_T$	$C_{p\_dw}$	$C_{p\_up}$	$q_{comp}$	$u(T)$	$u(p\_dw)$	$u(p\_up)$	$u(q)$	$ur(q)$	$ur(C_T)$	$ur(C_{p\_dw})$	$ur(C_{p\_up})$	$ur_{rep}$	$ur(q_{comp})$
			mol/s	°C	kPa	kPa	mol/s						
1.0143	1.0000	0.98296	9.596E-07	0.160	0.012	0.050	4.0E-09	4.2E-03	2.4E-03	1.0E-05	1.8E-04	2.0E-03	5.2E-03
1.0145	1.0000	0.99684	9.626E-07	0.160	0.012	0.050	4.0E-09	4.2E-03	2.4E-03	1.0E-05	1.8E-04	2.0E-03	5.2E-03
1.0123	1.0000	1.00483	9.631E-07	0.160	0.012	0.050	4.0E-09	4.2E-03	2.1E-03	1.0E-05	1.9E-04	2.0E-03	5.1E-03

## Leak L2, LNE

